Synthetic Aperture Sonar Nadir Gap Coverage with Centimetric Resolution

Jeremy Dillon, Shannon-Morgan Steele,
Richard Charron, David Shea, Nathan Smith
Kraken Robotic Systems Inc.
Mount Pearl, NL, Canada
{jdillon, ssteele, rcharron, dshea, nsmith}@krakenrobotics.com

Jan Albiez,
Alex Duda
Kraken Robotik GmbH
Bremen, Germany
{jalbiez, aduda}@krakenrobotik.de

***Abstract*—Synthetic aperture sonar (SAS) is an acoustic imaging technique capable of providing constant resolution over a wide swath. Similar to sidescan sonar, SAS has a coverage gap directly below the system known as the nadir gap. Developing nadir gap coverage technologies for SAS is challenging because it is difficult to match its altitude and resolution capabilities. In this paper, we introduce a unique gap reduction technique that combines a short-range SAS designed to reduce the nadir gap, with an auxiliary sensor to provide complete nadir gap coverage. Two different auxiliary sensors are investigated: a 3D laser profiler and a multibeam echosounder. Results indicate that all three gap fill solutions are capable of providing high (centimetric) resolution for a high speed towed SAS system operating at 10 m altitude. When combined, the sensors can provide full swath coverage that results in a 33% increase in area coverage rate.**

***Index Terms*—synthetic aperture sonar, sonar imaging, laser imaging, nadir gap filler, multibeam echo sounder**

I. Introduction

Side-looking imaging sonars map the seabed by transmitting acoustic pulses and processing the backscattered signals. In the across-track direction, centimetric resolution is obtained using a wideband pulse, such as a linear frequency-modulated chirp, with a bandwidth of several tens of kilohertz. Although across-track resolution is constant in slant range coordinates, resolution deteriorates near nadir when imagery is projected onto the seafloor. Furthermore, side-looking systems are often designed with narrow vertical beams to mitigate multipath interference in shallow water [1], in which case there is no acoustic return from the seabed in the nadir region. While surveying a large area, for example with a lawnmower pattern, gaps may be eliminated using overlapping tracks with a corresponding reduction in area coverage rate. However, for applications such as mine countermeasures and pipeline surveying, it is often desirable to perform single-pass coverage while filling the nadir gap with centimetric resolution.

The gap fill problem is especially challenging for high resolution side-looking Synthetic Aperture Sonar (SAS). For SAS, the along-track motion of the sensor platform is used to synthesize an aperture with a length that increases with range, thereby achieving constant centimetric resolution in both the along-track and across-track directions. Because SAS resolution is independent of frequency, extremely high area coverage rates are realized by operating at lower frequencies than conventional sidescan sonar to reduce acoustic absorption. As a result, SAS systems are typically operated at altitudes of 10–30 m with near-range imagery beginning at depression angles up to approximately $45°$, leaving a double-sided nadir gap of at least two times altitude. The combination of relatively high altitude and a nadir gap with angular extent of at least $90°$ implies that there are no commercially available sensors that can fill the gap with centimetric resolution comparable to SAS [2].

Fig. 1. KATFISH™ actively controlled towfish with AquaPix® Miniature Interferometric Synthetic Aperture Sonar (MINSAS).

In this paper, we describe and demonstrate the capabilities of a unique gap reduction technique for KATFISH™ (shown in Figure 1), an actively controlled smart towfish with SAS imaging, bathymetry, and navigation sensors. KATFISH also includes a launch and recovery system, an operator console, and real-time visualization software. One advantage of towed systems is that they achieve high area coverage rates at low altitude by increasing the survey speed compared to self-propelled Autonomous Underwater Vehicles (AUVs). The KATFISH nadir gap solution combines a short-range SAS and auxiliary sensors to provide complete nadir gap coverage. Two auxiliary sensors are used for filling the remain-

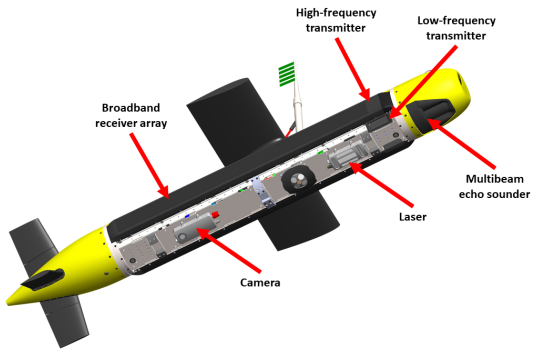

Fig. 2. Rendering of KATFISH equipped with both the high-frequency (long-range) and low-frequency (short-range) SAS, as well as two auxiliary gap fill sensors: the SeaVision 3D laser profiler (laser and camera), and a multibeam echo sounder.

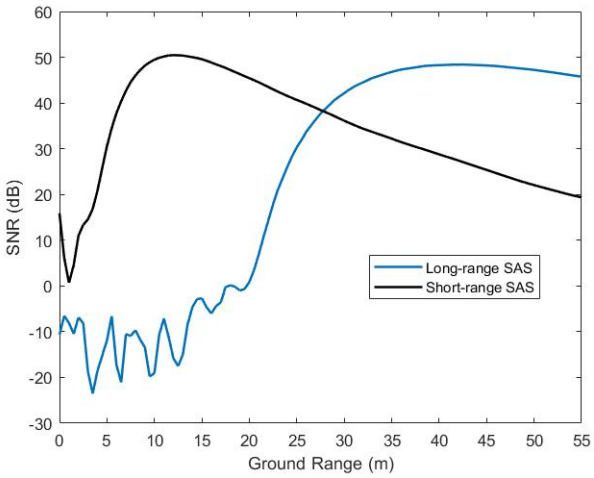

Fig. 3. Sonar performance models of the short and long range SAS at 10 m altitude.

der of the nadir gap left after short-range SAS processing: Kraken's SeaVision® 3D laser profiling system capable of sub-centimeter resolution, and a multibeam echo sounder with along-track resolution on the order of tens of centimeters. The integration of the sensors in the tow body is shown in Figure 2.

In Section II, we derive the area coverage rates for a SAS with and without gap fill techniques and assess the impact of nadir gap size on the efficiency of a survey mission. Section III presents performance predictions and results from Kraken's novel short-range SAS gap reducer for the KATFISH. Section IV evaluates laser and multibeam echosounder technologies for filling the remainder of the nadir gap with an assessment of the resolution and trade-offs associated with each approach. Experimental results are presented for Kraken's SeaVision 3D laser profiler.

II. Area Coverage Rate

One of the fundamental constraints of forming a synthetic aperture is that the ping-to-ping displacement must not exceed half the length of the receiver array L_R. For a pulse repetition interval T, the speed V of the vehicle is therefore limited to

$$V \leq \frac{L_R}{2T}. \tag{1}$$

To avoid range ambiguities, the maximum range R of the sonar is limited by the two-way propagation time of the acoustic pulse, resulting in

$$R \leq \frac{CT}{2} \tag{2}$$

where C is the speed of sound. The theoretical maximum Area Coverage Rate (ACR) of a dual-sided SAS is therefore

$$ACR = 2VR \leq \frac{CL_R}{2}. \tag{3}$$

Equation (3) shows that SAS ACR is fundamentally controlled by the length of the receiver array, allowing a trade-off between speed and maximum range to achieve the survey objectives. The result in (3) neglects the small ping-to-ping overlap necessary for SAS motion estimation, a range reduction of $C\tau/2$ for matched filtering an acoustic pulse of duration τ, and the nadir gap inherent in a side-looking survey geometry.

The primary motivation for gap fill technology is to maximize the ACR while maintaining centimetric resolution comparable to SAS, which is necessary for many applications of seabed mapping. Full area coverage is strictly required for many survey applications such as mine hunting [3] or hydrographic surveying [4]. To obtain full search area coverage, side looking sonars without gap fill technology must survey in a lawnmower fashion, where even and odd-numbered lines cover each other's gap [5]. Operating in this fashion decreases the ACR, where the decrease depends on the size of the gap and the overlap of the lines. We can calculate an upper bound on the ACR with a nadir gap by computing the ACR for the case where there is minimal overlap amongst the lines [5]:

$$ACR = \frac{(3R - r)}{2} V \tag{4}$$

where r is the minimum operating range of the SAS. It is assumed that $r \leq R/3$ to ensure that the gap is completely filled by a second pass. With overlapping survey lines, some portions of the seabed are mapped twice. The percent coverage PC is

$$PC = 100\,\frac{4(R - r)}{3R - r}, \tag{5}$$

which varies between 100% and 133% depending on the size of the gap.

The above expressions are valid for $r \leq R/3$, which is typical for systems with a moderately sized gap. However, some combinations of altitude and speed may result in a minimum range that exceeds $R/3$. For example, if both altitude and speed are simultaneously large, r is proportional to altitude whereas R is inversely proportional to speed, since R is limited by the pulse repetition interval necessary to maintain a ping-to-ping displacement less than $L_R/2$ in (1) and (2).

In general, the number of passes N required to fill the gap is given by

$$N = \left\lceil \frac{2r}{R-r} \right\rceil \tag{6}$$

where $\lceil x \rceil$ is the smallest integer greater than or equal to x. The general formulas for ACR and PC are

$$ACR = \frac{2R + N(R-r)}{N+1} V, \tag{7}$$

$$PC = 100\,\frac{2(N+1)(R-r)}{2R + N(R-r)} \tag{8}$$

which reduce to (4) and (5) in the case where $N = 1$.

In (4), it is seen that in the limit $r \to 0$, the ACR is limited to $1.5VR$ compared to $2VR$ in (3) for the case with no gap. Thus, the presence of any nadir gap causes a minimum 25% reduction in ACR. Adding a nadir gap fill sensor therefore increases the ACR by at least 33% compared to a system using overlapping passes to achieve full coverage. The actual size of the gap is relatively unimportant since r is much less than $3R$ in practice.

III. Gap Reduction with Short-Range SAS

The short-range SAS solution utilizes an additional transmitter operated at lower frequency (105 kHz) with a relatively wide vertical beampattern. Using a wide transmit beam in the vertical plane can cause severe multipath interference in shallow water. We minimize the impact of multipath by mounting the transmitter at a much larger depression angle ($45°$), thus directing more sound downwards, and by ignoring the low frequency sonar echoes at long range where multipath contamination may occur. The short-range SAS signals are recorded and digitized simultaneously with the long-range SAS using a single wideband receiver array. Therefore, the short-range SAS adds minimal complexity to the sensor platform and requires no new processing chain other than basebanding and demodulation of a second data stream. By using the short-range SAS, the angular extent of the nadir gap is reduced to $60°$ while maintaining the same along-track resolution of the long-range SAS, as shown in Figure 4b.

The model described in [6] and [7] was used to compare the range performance of both the short-range and long-range SAS. Measured transmitter and receiver beampatterns were used as inputs to the model. For this example, we have chosen a deep water environment (70 m water depth) with the platform flying at an altitude of 10 m above the seabed. The seabed type chosen for this model is a silt sediment. The long-range SAS (MINSAS), has an approximate starting ground range of around 20 m based on the rise in seabed backscatter shown in Figure 3. The short-range SAS has a wider transmit beam and significantly larger depression angle, giving it a starting range of 6 m and an ending range around 40 m. The SNR performance envelopes of the two SAS systems cross over at a range of approximately 27 m. The short-range SAS can therefore reduce the nadir gap by covering the imaging gap from 6 m range (0.6X altitude) to where the long-range SAS begins at 20 m range (2X altitude).

Unlike conventional sidescan sonar and multibeam echosounders, SAS along-track resolution is frequency independent and constant with range [8]. The short-range SAS is designed to maintain the 3.3 cm along-track resolution achieved by the long-range SAS, as shown in Figure 5. For SAS, the along-track resolution δ_x is determined by the length L_T of the transmitter element [9]

$$\delta_x = \frac{L_T}{2}. \tag{9}$$

In the across-track direction, resolution is determined by the bandwidth of the acoustic pulse. There is a loss of resolution in the near range. The across-track resolution δ_y is given by

$$\delta_y = \frac{C}{2B \sin\theta} \tag{10}$$

where B is the signal bandwidth and θ is the elevation angle from a point on the seabed to the sonar. Equation (10) demonstrates that side looking systems have a data quality gap near nadir, since θ approaches zero directly below the vehicle.

Currently, KATFISH is equipped with a low-frequency transmitter with a bandwidth of 20 kHz. The short-range SAS across-track resolution is approximately 4–7 cm, as shown in Figure 5. In the near future, the short-range SAS bandwidth will be increased to 40 kHz, which will provide 2–3.5 cm across-track resolution for gap reduction, thereby filling the gap with a resolution comparable to the long-range SAS.

IV. Nadir Gap Coverage with Auxiliary Sensors

A. Laser Imaging

Underwater optical sensing has a long history in the underwater community, and its fundamental limits due to the absorption and scattering properties of the surrounding medium water were already established in the 1960s by [10]. As a result, the best performance can be expected for active systems combining a narrow field-of-view for the source and, at the same time, for the receiver element minimizing the common volume between the illumination beam and the receiver. This particular setup reduces back- and forward scatter by a spatial rejection of light from the outside of this volume. Here, a standard illumination method for underwater 3D sensing is the usage of line patterns, which can be generated with high precision and optical power using laser diodes. This method is for example used by [11]–[15] to triangulate underwater 3D scene points intersected by the known active line pattern.

The underlying principle of these so-called line structured light systems is adopted by the commercially available SeaVision system, shown in Figure 6, and its derived 3D Profiler. SeaVision is a flexible platform that maintains maximal performance under given environmental conditions. For this, SeaVision consists of two identical daisy-chainable pressure housings with flexible mounting options to meet mission requirements with a customized baseline from 0.3 m to 3 m.

Each of the two compartments consists of the following components:

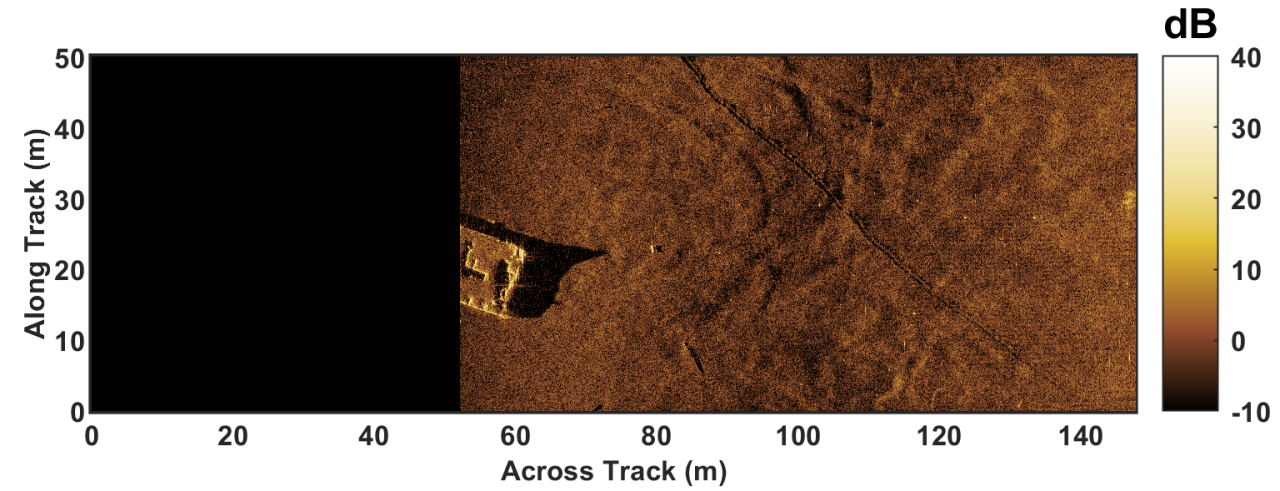

(a) MINSAS (long-range SAS), with nadir gap shown in black.

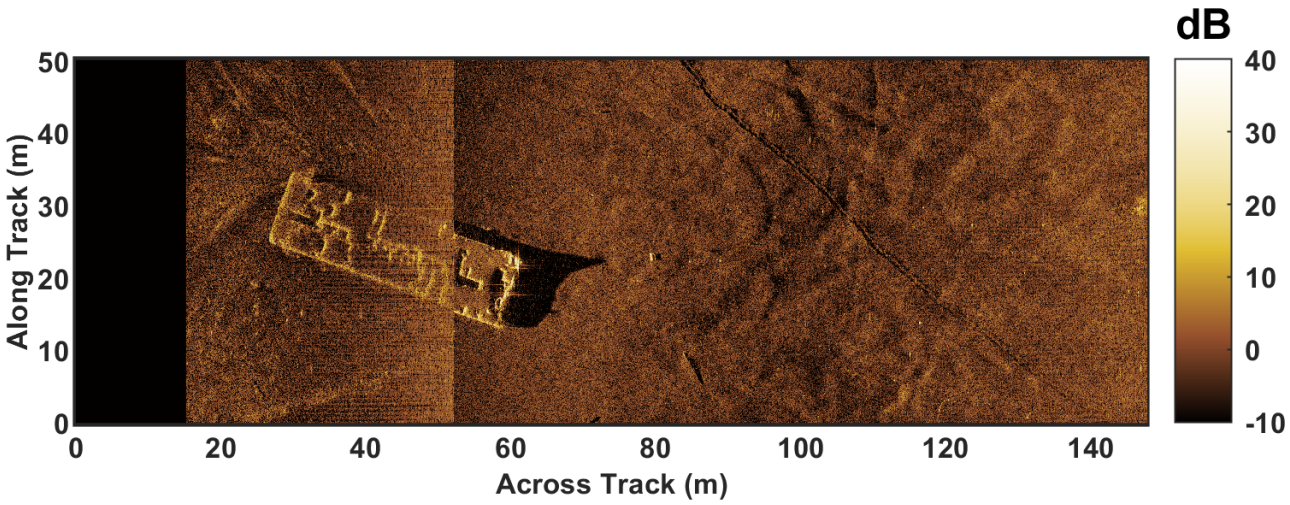

(b) MINSAS (long-range SAS) and short-range SAS images superimposed, with remaining nadir gap shown in black.

Fig. 4. Comparison of the nadir gap without (a) and with (b) short-range SAS gap reduction.

- High-speed, low light camera
- Embedded PC with GPU
- Microcontroller
- RGBW flashlight
- Servo
- Three lasers (red, green, and blue)

The embedded servo can sweep the lasers across the scene while the carrier system is hovering or steer them to an optimal angle for profiling. Each camera is electronically synchronized to the laser of the other compartment and forms an independent line structured light system. Therefore, a standard SeaVision system consists of two independent line structured light systems with three steerable line-lasers each. Additional configurations are possible by adding more SeaVision compartments to the setup to build, for example, a three pod system to measure undercuts. This flexible and independent design allows for supporting all major line structured light configurations with minimal software and hardware adaptions. Here, a derived system is, for example, a high power profiler using an additional external laser, extending the range of the standard system to around 10 m.

In the case of the KATFISH, its embedded laser profiler is a derived high power profiler stripped down to the bare minimum to reduce its impact on the vehicle dynamics during

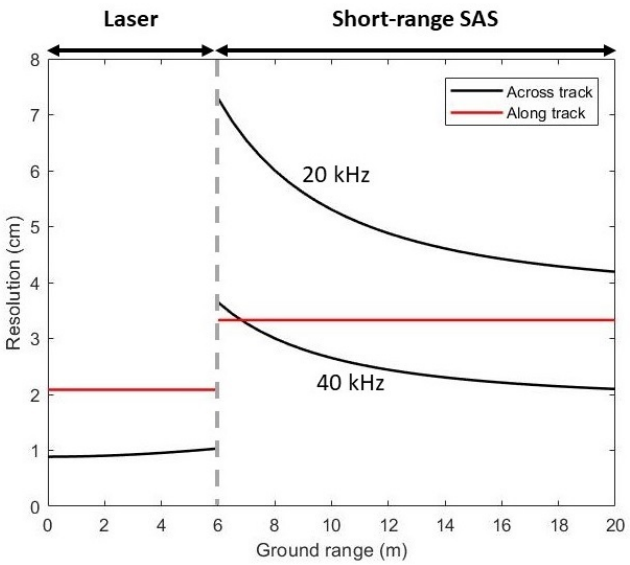

Fig. 5. Laser scanner and short-range SAS resolution as a function of ground range. Short-range SAS resolution depends on whether the system has 20 kHz of bandwidth or 40 kHz of bandwidth.

Fig. 6. SeaVision pressure housing pods.

high-speed surveys. It also consists of two compartments. However, the first one only houses a 500 mW green line laser and a microcontroller while the other one is equivalent to a single SeaVision compartment containing a camera and running the same software stack but without steerable light emitters.

These modifications allow the use of the SeaVision as an ultra-high resolution gap filler for the KATFISH. Due to the stability of the vehicle in combination with SeaVision's low light camera supporting frame rates of more than 120 fps, the resulting laser profiler matches or exceeds the resolution of the SAS system in both the along- and across-track directions, even during high-speed surveys. The impact of towing speed on the 3D resolution of the laser profiler has been validated

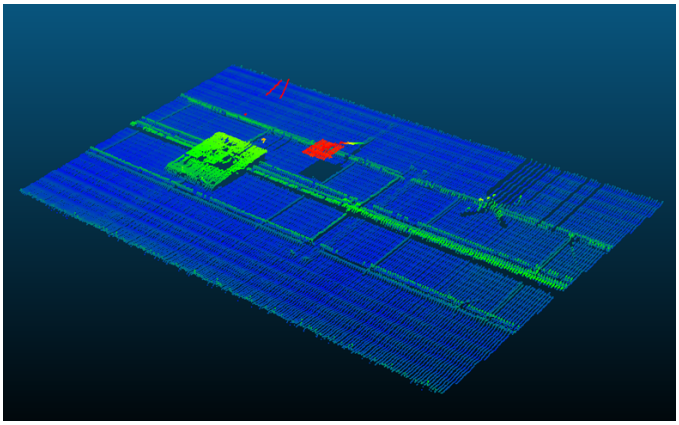

Fig. 7. SeaVision scan of a plate, cube, and sonar target at 7 m range while towing at 5 m/s

with multiple tests conducted in a 200 m long, 7 m deep, and 12 m wide towing tank located in St. John's, Canada. During these tests the SeaVision profiled objects sitting on the tank floor at a range of 7 m, as shown in Figure 7. While towing at maximal KATFISH speeds (up to 5 m/s), the SeaVision maintained along-track resolutions of less than 3.5 cm with a dimensional accuracy better than 0.018 cm. The SeaVision also supports sub-centimeter mapping for pre-selected seabed patches surveyed from low altitudes with reduced towing speeds.

Similar to SAS, the SeaVision maintains constant along-track resolution with ground range, as indicated in Figure 5. The along-track resolution of the SeaVision can be calculated as the platform speed divided by the frame rate. The maximum frame rate of the SeaVision is 144 Hz and here we have assumed a common towed platform speed of 3 m/s. The across-track resolution of the SeaVision is dependent on the slant range SR, the field of view FOV in radians, and the number of pixels N in the across-track direction:

$$\delta_y = SR\,\frac{FOV}{N}. \tag{11}$$

Therefore, the laser across-track resolution has a slight ground range dependency in Figure 5 due to the conversion between slant range and ground range. The SeaVision has a maximum FOV of 65° and 1280 pixels.

B. Multibeam Echosounder

In cases where the system is required to fly at high altitudes (above 10 m) or when operating in areas with significant turbidity, it may be more practical to use a multibeam echosounder (MBES) as the nadir gap filler instead of the laser profiler. The KATFISH is equipped with a NORBIT iWBMS multibeam echosounder that can be used for hydrography as well as a gap filler for the side-looking SAS. This MBES operates at a nominal frequency of 700 kHz with 80 kHz bandwidth. With this configuration, the MBES along-track beamwidth β is 1.0° and the across-track beamwidth ϕ is 0.5°.

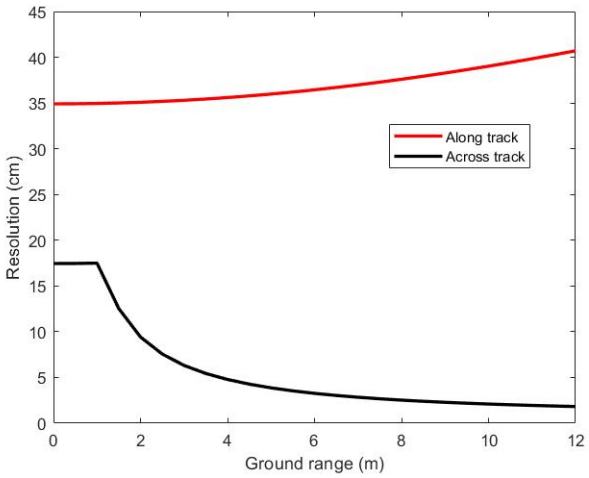

Fig. 8. Along-track and across-track multibeam echosounder resolution at 20 m altitude.

The MBES footprint is dependent on the altitude h above the seabed [16].

The along-track resolution is given by

$$\delta_x = h \sec\theta \sin\beta. \tag{12}$$

Along-track resolution increases slightly with ground range, as shown in Figure 8, and has significantly lower resolution than the across-track direction.

The across-track resolution is dependent on whether the instantaneous ensonified area is bandwidth or beamwidth limited [17]. Near nadir, the projected bandwidth is greater than the projected across-track beam footprint, and thus the resolution is beamwidth limited, given by

$$\delta_y = h \sec^2\theta \sin\phi. \tag{13}$$

Away from nadir, the projected bandwidth becomes smaller than the across-track beam footprint, and thus the across-track resolution can be computed in the same manner as SAS using (10). An example of the ground range dependency of the NORBIT iWBMS multibeam resolution is shown in Figure 8. At an altitude of 20 m, the across-track resolution is beamwidth limited up to 1 m of ground range, then it becomes bandwidth limited.

V. Conclusion

In addition to increasing the ACR, gap fill technology simplifies the mission planning process by eliminating the requirement for overlapping survey lines. Using a lower frequency transmitter for short-range SAS is an enabling technology for maximizing the single-pass area coverage rate with minimal additional hardware complexity and centimetric resolution across the entire swath. The presented results indicate that significant ACR gains can be achieved by using an auxiliary sensor such as a laser profiler or multibeam echosounder to fill the remainder of the gap. The laser scanner is the preferred auxiliary sensor option due to its ability to maintain or surpass SAS resolution; however, some operating conditions such as high altitude surveying and high turbidity may require use of acoustic sensors instead. Although auxiliary sensors add some complexity and expense to the platform, their expense is justified by the fact that they improve efficiency and have additional purposes. For example, a multibeam echosounder is often already installed on many platforms for hydrographic applications. Similarly, the laser profiler can also be used for detailed inspections and target identification. We have demonstrated that short-range SAS gap reduction combined with commercially available auxiliary sensors can achieve an increase in area coverage rate of 33% while maintaining centimetric resolution across the entire swath.

References

[1] M. Pinto, "Interferometric synthetic aperture sonar design optimized for high area coverage shallow water bathymetric survey," *Proc. 4th International Conference and Exhibition on Underwater Acoustic Measurements*, 2011.

[2] P. E. Hagen, "Gap filler sensors for SAS," *MTS/IEEE OCEANS Kona*, 2011.

[3] F. Florin, F. Fohanno, I. Quidu, and J. P. Malkasse, "Synthetic aperture and 3D imaging for mine hunting sonar," *Undersea Defence Technology (UDT) Europe*, 2004.

[4] *IHO Standard for Hydrographic Surveys, Spec. Publ., 44*, 1996.

[5] P. E. Hagen and R. E. Hansen, "Area coverage rate of synthetic aperture sonars," *OCEANS Europe*, 2007.

[6] S.-M. Steele, R. Charron, J. Dillon, and D. Shea, "Shallow water survey with a miniature synthetic aperture sonar," *MTS/IEEE OCEANS Seattle*, 2019.

[7] ——, "Performance prediction for a low frequency ultra-wideband synthetic aperture sonar," *MTS/IEEE OCEANS Seattle*, 2019.

[8] L. J. Cutrona, "Additional characteristics of synthetic-aperture sonar systems and a further comparison with nonsynthetic-aperture sonar systems," *The Journal of the Acoustical Society of America*, vol. 61, no. 5, pp. 1213–1217, 1977.

[9] J. Dillon and R. Charron, "Resolution measurement for synthetic aperture sonar," *MTS/IEEE OCEANS Seattle*, 2019.

[10] S. Q. Duntley, "Light in the sea," *Journal of the Optical Society of America*, vol. 53, no. 2, p. 214, Jan 1963.

[11] J. Klepsvik, H. Torsen, and K. Thoresen, "Laser imaging technology for subsea inspection: Principles and applications," *IRM incorporating ROV 90*, 1990.

[12] C. Roman, G. Inglis, and J. Rutter, "Application of structured light imaging for high resolution mapping of underwater archaeological sites," *IEEE OCEANS Sydney*, 2010.

[13] J. Liu, A. Jakas, A. Al-Obaidi, and Y. Liu, "Practical issues and development of underwater 3D laser scanners," *2010 IEEE 15th Conference on Emerging Technologies & Factory Automation (ETFA 2010)*, 2010.

[14] J. Albiez, A. Duda, M. Fritsche, F. Rehrmann, and F. Kirchner, "CSurvey—An autonomous optical inspection head for AUVs," *Robotics and Autonomous Systems*, vol. 67, pp. 72–79, 2015.

[15] J. V. D. Lucht, M. Bleier, F. Leutert, K. Schilling, and A. Nüchter, "Structured-light based 3D laser scanning of semi-submerged structures," *ISPRS Annals of Photogrammetry, Remote Sensing and Spatial Information Sciences*, vol. IV-2, pp. 287–294, 2018.

[16] L. Hellequin, J.-M. Boucher, and X. Lurton, "Processing of high-frequency multibeam echo sounder data for seafloor characterization," *IEEE Journal of Oceanic Engineering*, vol. 28, no. 1, pp. 78–89, 2003.

[17] R. J. Urick, "The backscattering of sound from a harbor bottom," *The Journal of the Acoustical Society of America*, vol. 26, no. 1, p. 148, 1954.